Compound sawtooth in EAST LHCD plasma: An experimental study*

Xu Li-Qing(徐立清)†, Hu Li-Qun(胡立群), Chen Kai-Yun(陈开云), and Li Miao-Hui(李妙辉)

Institute of Plasma Physics, Chinese Academy of Sciences, Hefei 230031, *China*

(Received 17 October 2013; revised manuscript received 6 March 2014; published online 10 June 2014)

A compound sawtooth with an incomplete relaxation was observed in EAST's lower hybrid current drive (LHCD) plasma. The sub-crash phase of the compound sawtooth corresponds to a longer-lasting and slower-growing 1/1 mode. Based on the two-dimensional (2D) SXR tomography, the time-dependent 2D image of a compound sawtooth crash is obtained. The island produced during a resistive internal kink mode is observed in the all crash phases of the compound sawtooth. The destabilization of 1/1 long-lasting saturated 1/1 mode is related to the current driven by the LHCD near the $q = 1$ surface.

Keywords: compound sawtooth, EAST, LHCD plasma

PACS: 52.35.Py, 52.70.La, 52.55.Tn, 52.55.Fa **DOI:** 10.1088/1674-1056/23/8/085201

1. Introduction and motivation

Tokamak plasmas are observed to be highly sensitive to a variety of large-scale instabilities, which can degrade the plasma confinement. The safe operating regime of the tokamaks is governed by the stability boundaries of these large plasma instabilities.[1] Thus, the understanding of the formation and stability of such a macroscopic mode in the core of the axisymmetric toroidal configuration is one of the challenges of current fusion research. One of the most interesting and commonly observed examples of such large-scale magnetohydrodynamic (MHD) perturbations in the core of a tokamak is the sawtooth oscillation found at ST[2] nearly four decades ago. The typical sawtooth cycle consists of a quiescent period, during which the plasma density and temperature increase, followed by the growth of a helical magnetic perturbation, which in turn is followed by a rapid collapse of the central density and temperature.[3] A special type of sawtooth oscillation, the compound sawtooth,[4–6] consists of an incomplete relaxation after approximately one normal sawtooth period, followed by a large 'main collapse' one period later.[7] The large collapse of a compound sawtooth can supply a seed island [8–11] for the neo-classical tearing mode (NTM). It is potentially important to understand the close relationship between these phenomena and the sawtooth for ITER where the $q = 1$ radius can be as large as half the minor radius.

The first theoretical sawtooth model, which was known as the complete reconnection model, was proposed by Kadomtsev.[12] However, the Kadomtsev model cannot explain all of the later experimental observations about sawtooth crashes. Subsequently, fast reconnection models in collisionless regimes were proposed by considering electron inertia,[13,14] Hall effects,[15] and other non-ideal kinetic effects in the thin current layer. Up to now, the crash mechanism is still an insoluble mystery. However, there is no doubt that the linear growth[16] and nonlinear evolution ($m = 1$ stability) of the $m = 1$ precursor play vital roles in the sawtooth crash, especially in the compound sawtooth crash.

This paper reports experimental data on the $m = 1$ behaviors in a compound sawtooth in the EAST lower hybrid current drive (LHCD) plasma. The evolution of the compound sawtooth pictures will be presented by means of tomography of a multi-array and high-resolution soft X-ray system. In addition, the role of the stability of the $m = 1$ precursor to the period and amplitude of the compound sawtooth is analyzed.

This paper is arranged as follows: in Sections 2 and 3 we discuss the diagnostic tools used in EAST, as well as describing the details of the dynamic evolution of compound sawtooth instability. A summary and future work can be found in section 4.

2. Description of the diagnostics used for the characterization of a sawtooth

EAST is a superconducting tokamak with major radius $R_0 = 1.70$ m, minor radius $a = 0.40$ m, toroidal magnetic field $B_T < 3$ T, plasma current $I_p \leq 1$ MA, and elongation ratio $\kappa = 1.8$–2. It was designed for long-pulse diverter operations up to 1000 s[17,18] and achieved diverter discharges exceeding 400 s during the last experimental campaign. The

*Project partially supported by the JSPS-NRF-NSFCA3 Foresight Program in the Field of Plasma Physics (NSFC) (Grant No. 11261140328) and the National Natural Science Foundation of China (Grant No. 10935004).

†Corresponding author. E-mail: lqxu@ipp.cas.cn

© 2014 Chinese Physical Society and IOP Publishing Ltd

X-ray tomographic system used extensively for this paper is located in port C, and the line arrangement is shown in Fig. 1. Each of the horizontal arrays (U and D) has 35 chords, and the vertical array V has 46 chords. The chords used to identify the compound sawtooth location appear highlighted and numbered. The SXR diodes are filtered using 12.5-μm beryllium foils. The spatial resolution is 2.5 cm in the central region.[19] The maximum sampling rate is 100 kHz, which is enough to resolve sawtooth precursors since their toroidal frequency is on the order of a few kHz.

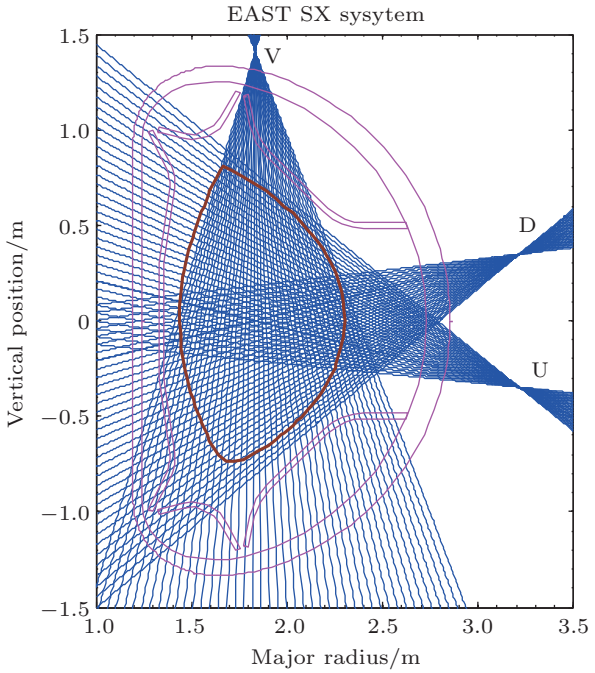


Fig. 1. (color online) The soft X-ray tomographic system in EAST. The U and D arrays each have 35 chords that are numbered clockwise from 1 to 35. V array has 46 chords named from SXC1V to SXC46V.

3. Typical compound sawtooth crash in EAST LHCD plasma

A compound sawtooth consists of an incomplete relaxation after approximately one normal sawtooth period, followed by a large 'main collapse' one period later. The main collapse of a compound sawtooth is comparable with a monster sawtooth[4,20] in amplitude. The main-crash of the compound sawtooth can trigger NTMs due to the seed island formation in the forced magnetic reconnection process. A typical compound sawtooth crash in EAST LHCD discharge is shown in Fig. 2. Although the mechanism of a sawtooth crash is unclear now, there is no doubt that the stability of the $m = 1$ mode plays a vital role in the compound sawtooth crash. In EAST, the SVD method[21] is employed to extract the $m = 1$ mode from the total SXR signal, and the measured amplitude growth rate of the $m = 1$ precursor is estimated by exponential fit.[22] Figure 3(a) is a schematic plot of sawtooth amplitude δA and the saturated amplitude of $m = 1$ mode $A_{\rm sat}$. The small frame in the upper right of Fig. 3(a) is the raw data of the core SXR signal with impact parameter $Z = 0$ cm. Shown in Fig. 3(b) is the growth rate of $m = 1$ modes before the sub-crash and main-crash. The growth rate of the $m = 1$ mode ($\gamma \sim 160$ s^{-1}) before the sub-crash is much smaller than the one before the main-crash ($\gamma \sim 280$ s^{-1}). Figure 3(c) is a schematic map of the decay timescale of the $m = 1$ mode estimated from the time point of mode saturation to the exhaustion of the mode. Using the notation described in Fig. 3, a statistical analysis is used to study the $m = 1$ mode behaviors in a compound sawtooth crash. The statistical result about the $m = 1$ mode is shown in Fig. 4. Figure 4(a) indicates that a long lasting $m = 1$ mode always contributes to a longer period of sawtooth and the lifespan (li) of $m = 1$ in the sub-crash is longer than the one in the main-crash. As shown in Fig. 2(b), a larger amplitude of the $m = 1$ mode commonly leads to a bigger sawtooth crash and the amplitude of the sub-crash $m = 1$ mode is smaller than that of the main-crash one. The decay timescale of the $m = 1$ mode (see Fig. 3(c)) reflects the crash time scale of the sawtooth. From Fig. 4(c), it is clear that the crash of the main-crash is always faster than that of the sub-crash. The slower crashes in the sawtooth sub-crash are usually accompanied by longer decay timescales of the $m = 1$ mode. Comparing the lengths of the timescales of the $m = 1$ modes in a compound sawtooth and a normal sawtooth, it is clear that the one in a compound sawtooth is longer, as shown in Fig. 4(d).

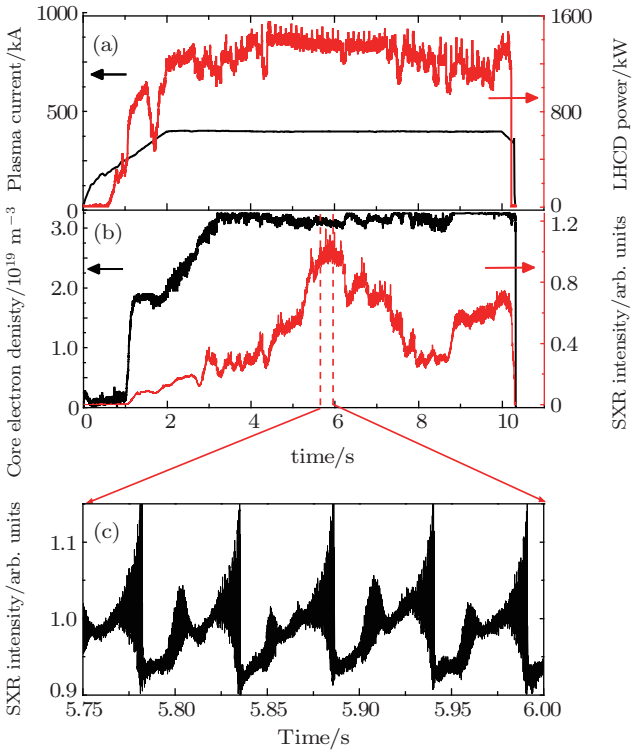


Fig. 2. (color online) Typical compound sawtooth crash in EAST LHCD shot #41360. In panel (a) the time traces show the auxiliary LHW power and the plasma current (in black). $P_{\rm LHW} = 1.3$ MW, $I_{\rm P} = 375$ kA. The time slices in panel (b) are the core SXR signal (in red) and the central line average electron density. $n_{\rm e} \approx 3 \times 10^{19}$ m^{-3}. (c) The expand core SXR signal with impact parameter $r = 0.27$ cm.

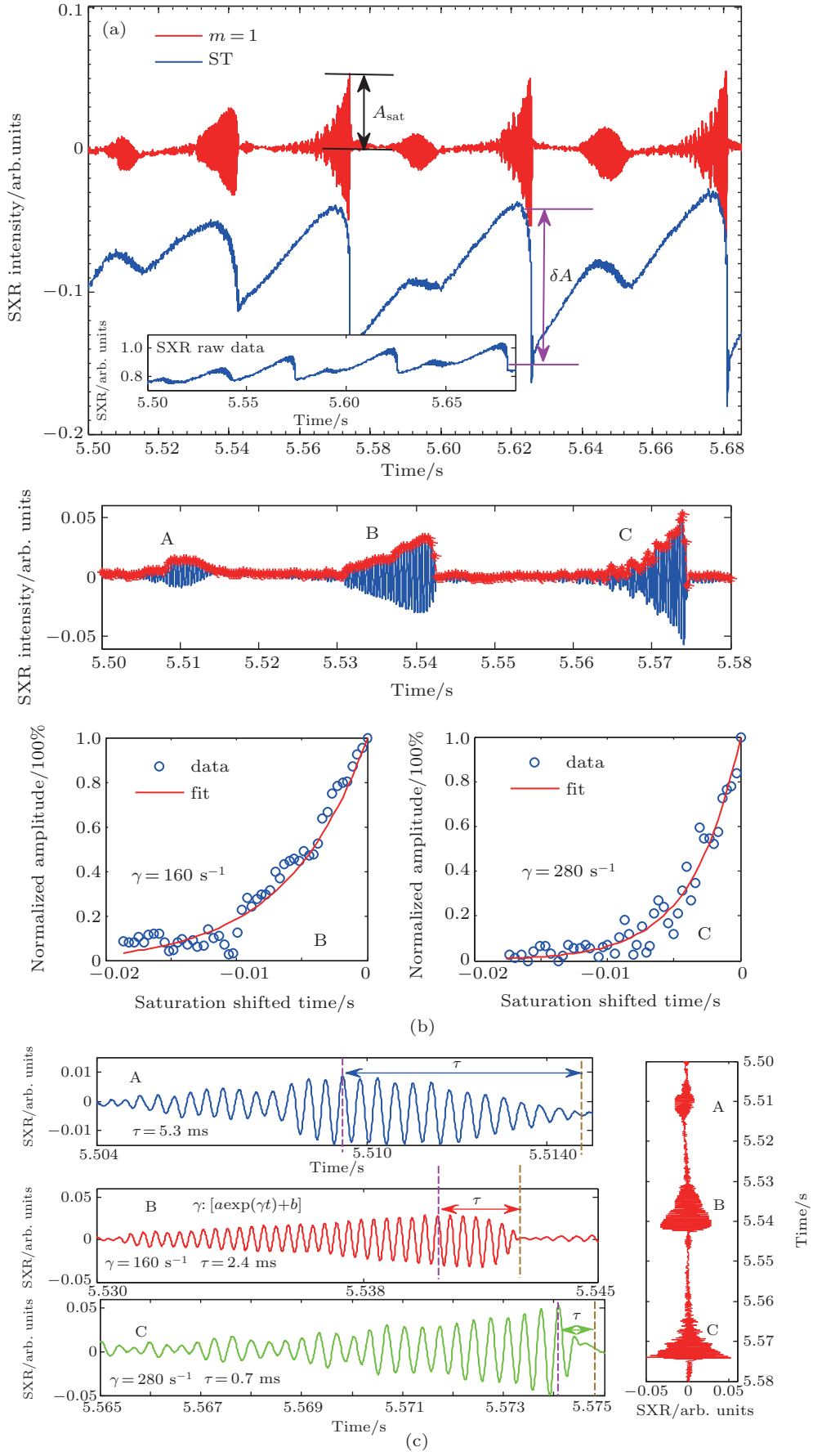


Fig. 3. (color online) SVD analysis of $m = 1$ in a compound sawtooth. (a) Schematic diagram of the amplitude of the $m = 1$ mode and the amplitude of the sawtooth. (b) Exponential fit of the growth rate of the $m = 1$ mode in the compound sawtooth. (c) Schematic diagram of the timescale of $m = 1$ damping. Fast growth of $m = 1$ in the larger sawtooth crash.

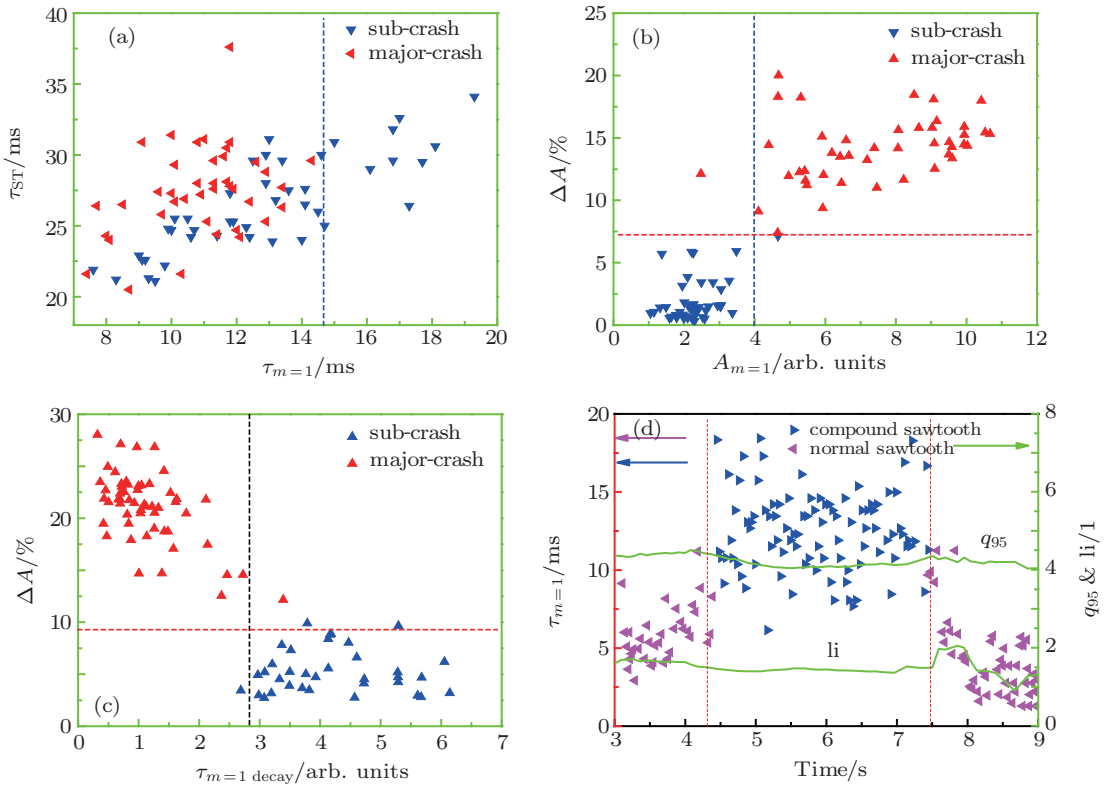


Fig. 4. (color online) Statistical results of $m = 1$ mode parameters in the compound sawtooth in EAST shot #41630. (a) Period of sawtooth τ_{ST} versus duration of $m = 1$ mode $\tau_{m=1}$. (b) Sawtooth amplitude ΔA versus amplitude of $m = 1$ mode $A_{sat_m=1}$. (c) Sawtooth amplitude ΔA versus decay timescale of $m = 1$ mode $\tau_{m=1}$. (d) Time evolution of the lasting time of $m = 1$ mode $\tau_{m=1}$.

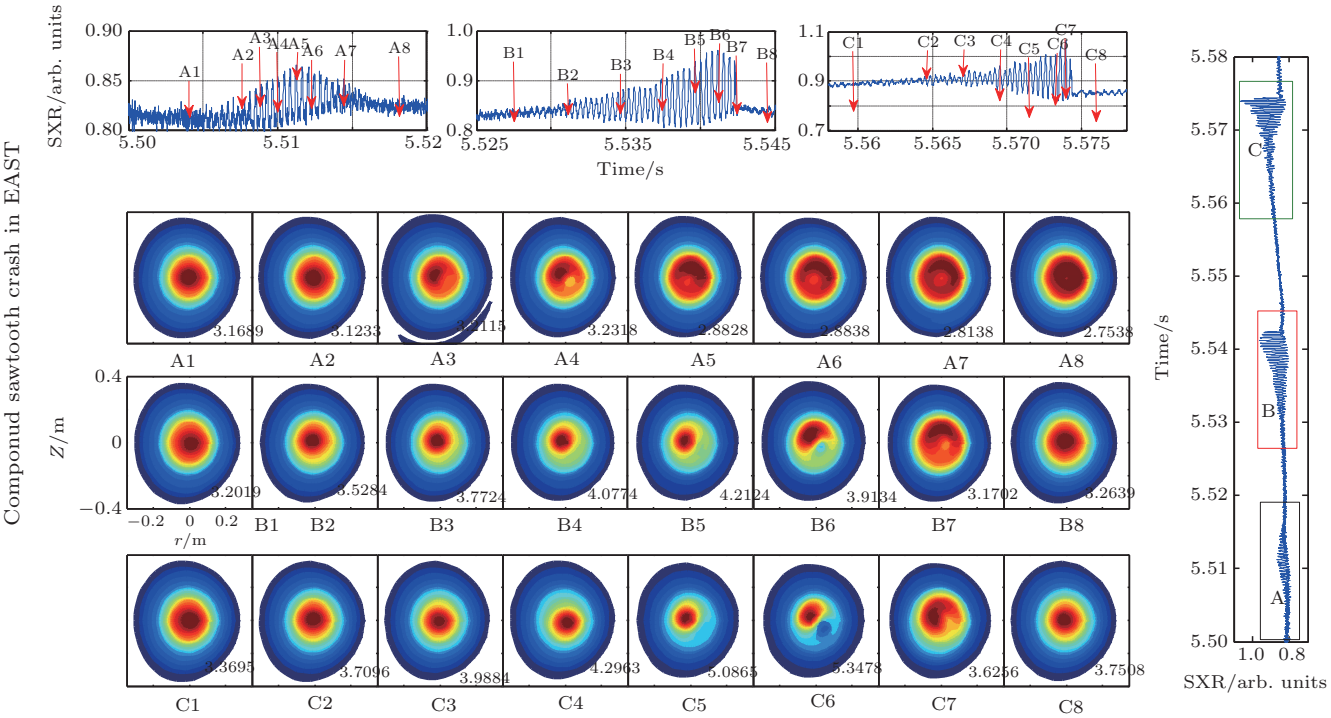


Fig. 5. (color online) Reconstructed compound sawtooth oscillations periodic pictures by using the tomography of SXR signals in shot #41630. The top row shows the evolution of the line-integrated soft X-ray signals at the central chord. The bottom three rows are the contour plots of the reconstructed local emission intensities profile from the total signals. The capital letters on the bottom of the reconstructed frames correspond to those in the top row frames.

Together with SVD method and SXR tomography, the crash pictures of compound sawooth oscillations are obtained. As shown in Figs. 5 and 6, before the sawtooth crash, including sub-crash and main-crash, the kink circular structures (A3, B4, and C3 of Fig. 5) are observed. During the crash phase, the initial broad kink-displacement transitions seamlessly into a crescent-shaped helical structure (A5, B6, and C7 of Fig. 5). The crescent-shaped helical structure fills the $q < 1$ region and resembles the

magnetic island produced during a resistive internal kink. It is clear that the magnetic reconnection occurs during the sawtooth crash phase. The difference between the main-crash and sub-crash is that the $m = 1$ mode still survives after the sub-collapse, shown in Fig. 6 (A6 and B7).

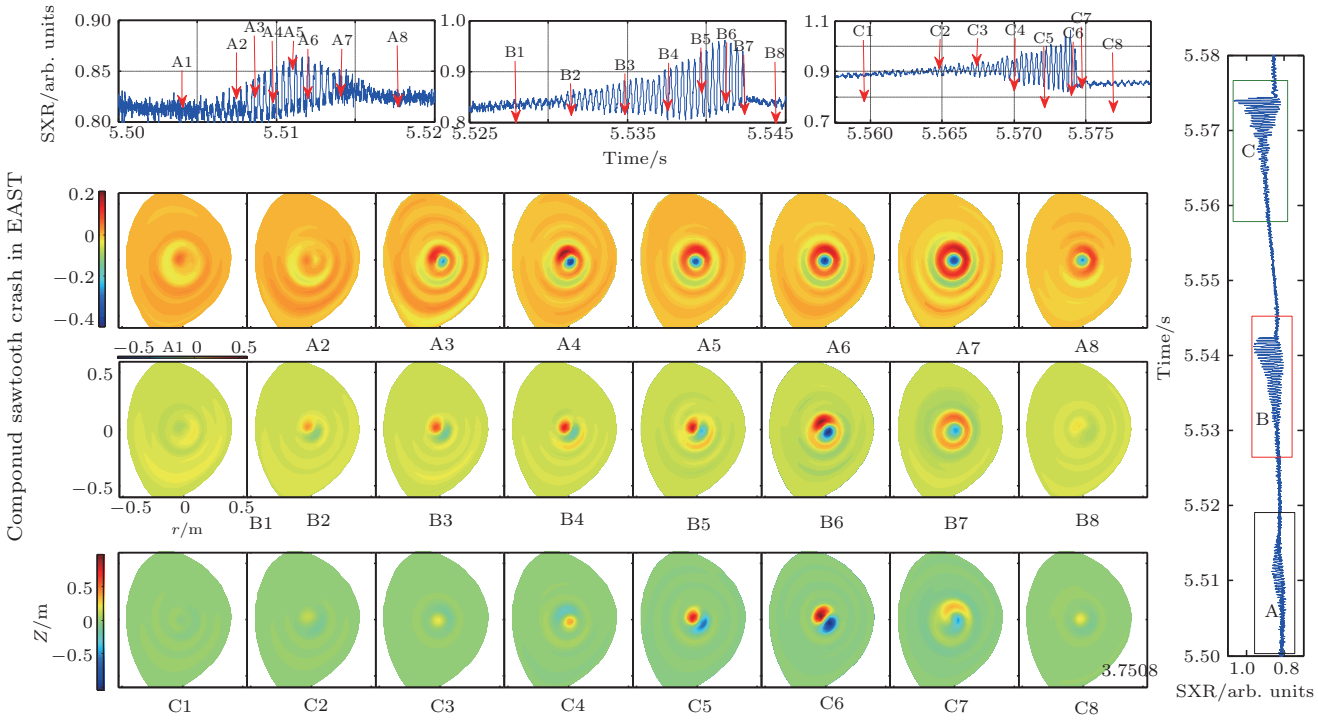


Fig. 6. (color online) Reconstructed $m = 1$ mode periodic pictures by the tomography of SXR signals in shot #41630. The bottom three rows are the contour plots of the reconstructed perturbation of the local emission intensities from the perturbation signals extracted by the SVD method. The capital letters on the bottom of the reconstructed frames correspond to those in the top row frames.

4. Conclusions and discussion

A compound sawtooth consists of more than one collapse and was observed in the EAST LHCD plasma. A long-lasting and slower growing 1/1 mode is commonly found in the sub-crash phase of a compound sawtooth. Based on 2D SXR tomography, the time-dependent 2D image of a compound sawtooth crash is investigated. The island produced during a resistive internal kink mode is observed in all the crash phases of the compound sawtooth. The $m = 1$ mode still survives after the sub-crash of the compound sawtooth. In EAST, the compound sawtooth can be found only in the LHCD plasma; this is because of the current driven by the LHCD located near the $q = 1$ surface. The LHCD driven current simulated by the C3PO/LUKE code confirms this fact, as shown in Fig. 7.

Many questions regarding sawtooth crash criteria, long-term survival $m = 1$ mode in the compound sawtooth, and interaction with other instabilities (e.g. with 'snakes') remain.

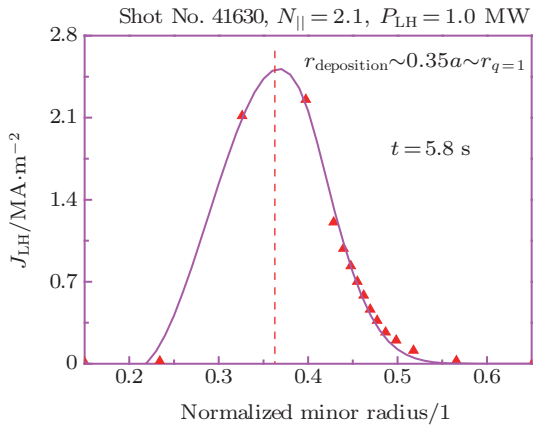


Fig. 7. (color online) Deposition of LHCD power near the $q = 1$ region. The current driven by the LHCD is calculated by the C3PO/LUKE code.

References

[1] Chapman I T 2011 *Plasma Phys. Control Fusion* **53** 013001

[2] Goeler S V, Stodiek W and Sauthoff N 1974 *Phys. Rev. Lett.* **33** 1201

[3] Chapman I T, Pinch S D, Graves J P, *et al.* 2007 *Plasma Phys. Control Fusion* **49** B385

[4] Pfeiffer W, Marcus F B, Armentrout C J, Jahns G L, Petrie T W and Stockdale R E 1985 *Nucl. Fusion* **25** 673

[5] Campbell D J, Gill R D, Wesson J A, Bartlett D V, Best C H, Coda S, Costley D V, Edwards A, Kissel S E, Niestatdt R M, Piekaar H W, Peentice P, Ross R T and Tubbing B J D 1986 *Nucl. Fusion* **26** 1085

[6] Westerhof W, Smeulders P and Cardozo N 1989 *Nucl. Fusion* **29** 1056

[7] Janick C, Simm C, Décoste R, Pacher G W and Pacher H D 1990 *Nucl. Fusion* **30** 950

[8] Sauter O, Westerhof E, Mayoral M L, *et al.* 2002 *Phys. Rev. Lett.* **88** 105001

[9] Ji X Q, Yang Q W, Liu Y, Zhou J, Feng B B and Yuan B S 2010 *Chin. Phys. Lett.* **27** 065202

[10] Shi T H, Wan B N, Shen B, Sun Y W, Qian J P, Hu L Q, Gong X Z, Liu G J, Luo Z P, Zhong G Q, Xu L Q, Zhang J Z, Lin S Y, Jie Y X, Wang F D and Lü B 2013 *Plasma Phys. Control Fusion* **55** 055007

[11] Xu L Q, Hu L Q, Chen K Y, Li E Z, Wang F D, Xu M, Duan Y M, Shi T H, Zhang J Z, Zhou R J and Chen Y B 2012 *Phys. Plasma* **19** 122504

[12] Kadomtsev B B 1975 *Sov. J. Plasma Phys.* **1** 389

[13] Porcelli F 1991 *Phys. Rev. Lett.* **66** 425

[14] Wesson J A 1990 *Nucl. Fusion* **30** 2545

[15] Wang X G and Bhattacharjee A 1995 *Phys. Plasmas* **2** 171

[16] Chapman I T, Hender T C, Saarelma S, Sharapov S E, Akers R J, Conway N J and MAST Team 2006 *Nucl. Fusion* **46** 1009

[17] Wan Y X 2000 *Nucl. Fusion* **40** 1057

[18] Wang H Q, Xu G S, Guo H Y, Wan B N, Naulin V, Ding S Y, Yan N, Zhang W, Liu S C, Chen R, Shao L M, Xiong H, Liu P, Jiang M and Luo G N 2012 *Nucl. Fusion* **52** 123011

[19] Chen K Y, Hu L Q, Chen Y B, Ma T P and Duan Y M 2010 *Phys. Lett. A* **374** 1849

[20] Campbell D J, Start D F H and Wesson J A, *et al*. 1988 *Phys. Rev. Lett.* **60** 2148

[21] Sun Y W, Wan B N, Hu L Q, Chen K Y, Shen B and Mao J S 2009 *Plasma Phys. Control Fusion* **51** 065001

[22] Papp G, Pokol G I, Por G, Magyarkuti A, Lazanyi N, Horvath L, Igochine V and Marascheck M 2011 *Plasma Phys. Control Fusion* **53** 065007